LBL-28998
Preprint

Lawrence Berkeley Laboratory
UNIVERSITY OF CALIFORNIA

Materials & Chemical Sciences Division

Submitted to Physical Review B

Superconducting Vortex-Line Configurations in Materials with Twin Boundaries

H. Svensmark and L.M. Falicov

May 1990

For Reference

Not to be taken from this room

LBL-28998
Copy 1
Bldg. 50 Library.

Prepared for the U.S. Department of Energy under Contract Number DE-AC03-76SF00098.

DISCLAIMER

This document was prepared as an account of work sponsored by the United States Government. While this document is believed to contain correct information, neither the United States Government nor any agency thereof, nor the Regents of the University of California, nor any of their employees, makes any warranty, express or implied, or assumes any legal responsibility for the accuracy, completeness, or usefulness of any information, apparatus, product, or process disclosed, or represents that its use would not infringe privately owned rights. Reference herein to any specific commercial product, process, or service by its trade name, trademark, manufacturer, or otherwise, does not necessarily constitute or imply its endorsement, recommendation, or favoring by the United States Government or any agency thereof, or the Regents of the University of California. The views and opinions of authors expressed herein do not necessarily state or reflect those of the United States Government or any agency thereof or the Regents of the University of California.

LBL-28998

Superconducting Vortex-Line Configurations in Materials with Twin Boundaries

Henrik Svensmark and L.M. Falicov

Department of Physics
University of California

and

Materials and Chemical Sciences Division
Lawrence Berkeley Laboratory
University of California
Berkeley, CA 94720

This research was supported at the Lawrence Berkeley Laboratory, by the Director, Office of Energy Research, Office of Basic Energy Sciences, Materials Sciences Division, U.S. Department of Energy, under Contract No. DE-AC03-76SF00098.

Superconducting Vortex-Line Configurations in Materials with Twin Boundaries.

Henrik Svensmark and L.M. Falicov

Department of Physics, University of California, Berkeley, CA 94720,

and

Materials and Chemical Sciences Division, Lawrence Berkeley Laboratory,

Berkeley, CA 94720.

ABSTRACT

We have studied numerically the classical states of equilibrium, stable and metastable, of magnetic-field vortex lines in a type II superconductor in the presence of twin boundaries which attract the vortex lines. Depending on the value of the magnetic field and the density of the twin boundaries, a variety of situations is found. Among them are Abrikosov lattices, anisotropic structures in which the vortex lines are mostly localized at the twin boundaries, and a consistently large regime of disordered structures. Statistical analysis of the distributions, their energies, and their pair-correlation functions are presented.

Superconducting Vortex-Line Configurations in Materials with Twin Boundaries.

Henrik Svensmark and L.M. Falicov

Department of Physics, University of California, Berkeley, CA 94720,

and

Materials and Chemical Sciences Division, Lawrence Berkeley Laboratory,

Berkeley, CA 94720.

I. INTRODUCTION

In a type II superconductor it is expected that magnetic flux lines in equilibrium make an Abrikosov lattice, i.e. an ordered array with hexagonal symmetry [1–3]. Therefore it was somewhat surprising that decoration experiments on the new high-temperature superconductors exhibit hexagonal lattices only in some cases [4]. One of the first observations on a $YBa_2Cu_3O_{7-\delta}$ single crystal by Gammel *et al.* showed a considerably disordered lattice, though pair-correlation functions showed, on the average, hexagonal ordering [1]. Similar experiments on bismuth-based superconductors have shown a highly disordered flux lattice [5], as well as some indication that the flux lattice might melt. These findings have led to the speculation that new intrinsic

properties of the flux lines may be responsible for these unusual properties. The new features are believed to be caused by large fluctuations arising from a transition temperature T_c that is an order of magnitude larger than in traditional superconductors, and by a coherence length ξ which is an order of magnitude smaller. A consequence of such a view some authors believe that the flux lattice is no longer two-dimensional, and therefore three-dimensional effects have to be included in the description [6–8].

Aside from the possibility of fluctuation phenomena being important, the new materials all have a high concentration of defects. Since many of the decoration experiments exhibiting order/disorder are performed at low temperatures (4 K - 20 K) on *thin* single-crystal samples with the magnetic field perpendicular to the *ab*-plane, the third dimension (the thin dimension of the single-crystal film) along the *c*-axis is essentially frozen. Therefore it is likely that third-dimension fluctuations are not the primary cause of the observed disorder, and that in these thin samples the structure of the flux-line distribution is probably caused by crystalline defects which interact with the lines. The purpose of this contribution is to study the influence of a particular defect, the twin boundaries. Twin boundaries originate from the tetragonal-to-orthorhombic phase transition which many of the new high-temperature

superconductors undergo at various temperatures. The low-temperature orthorhombic phase, which consists of inequivalent *a* and *b* axes, seldom appears in "true" (untwinned) single crystals. In particular *YBaCuO* "single" crystals are normally highly twinned, with the twinning planes parallel to both the *c*-axis, and either the [1,1,0] or [-1,1,0] direction, *i.e.* they are (-1,1,0) or (1,1,0) planes.

Magnetic flux experiments[9,10] on *YBaCuO* "single crystals", with magnetic field parallel to the *c*-axis clearly show three regimes:

(1) in twin-free regions the flux lines, because of their mutual repulsion, distribute themselves in Abrikosov hexagonal lattices;

(2) twin boundaries act as an attractive potential for the flux lines, so that there are regions in which the flux lines localize themselves, almost exclusively, along the twin boundaries (planar anisotropic and possibly disordered arrangement);

(3) an intermediate regime where the attractive twin-boundary/flux-line interaction and the repulsive mutual interaction between the flux lines produce conflicting effects that result in a variety of glass-like disordered states, neither dominated by the twin boundaries (planar flux-line arrangement) nor ordered in a hexagonal,

defect-free lattice.

These three regimes are evident from an examination of, for instance, Figure 1 (a) of Ref. 9. A numerical study and an analysis of these regimes constitute the subject matter of this paper.

II. FORMULATION

Flux lines in type II superconductors are most conveniently described in the framework of Ginzburg-Landau (GL) theory [2]. In that theory the ratio $\kappa = \lambda/\xi$ of the magnetic penetration depth λ, and the coherence length ξ, plays a very important role. If κ is larger than $(1/\sqrt{2})$ the superconductor is called of type II: the magnetic field penetrates the superconductor in the form of quantized flux lines; each line contains one flux quantum $\Phi_0 = (hc/2e)$. For materials with large values of κ, the superconducting order parameter is constant over most of the sample, except in regions of the order ξ around the cores of the flux lines. Since in this work only interactions between flux lines in moderate fields are considered, it is a good approximation to neglect the "normal" cores of the flux lines, and use an order parameter of constant magnitude throughout the superconductor. In this limit the GL theory becomes

identical to the London theory[3], a considerable simplification of the problem. The magnetic field around a single flux line is thus given by

$$H(R) = \frac{\Phi_0}{2\pi\lambda^2} K_0(R/\lambda) \quad . \tag{1}$$

Here $H(R)$ is the local magnetic field at a radial distance R from the core of the line, Φ_0 is the magnetic flux quantum, and K_0 is the zeroth order Bessel function of the second kind. The contribution to the free energy arising from the interaction between flux lines is [3]

$$\Delta F_1 = \frac{(\Phi_0)^2}{8\pi^2\lambda^2} \sum_{i>j}^{N} K_0(R_{ij}/\lambda) \quad , \tag{2}$$

where R_{ij} is the separation between flux line i, located at $\vec{R}_i$, and line j, located at $\vec{R}_j$.

The presence of twin boundaries introduces and additional contribution to the flux-line free energy, a twin boundary potential ΔF_2. The total excess flux-line free energy -- caused by their mutual interaction and the interaction with the twin boundaries -- now becomes

$$\Delta F = \frac{(\Phi_0)^2}{8\pi^2\lambda^2} \sum_{i>j}^{N} K_0(R_{ij}/\lambda) - \sum_{i}^{N} V(\vec{R}_i) \quad . \tag{3}$$

The potential $V(\vec{R}_i)$ describes the attraction between the flux lines and the twin boundaries. An exponential potential was chosen to describe that interaction

$$V(\vec{R}_i) = V_0 \sum_k^{N_{twins}} \exp\left[\frac{-(X_i - x_k)^2}{\sigma^2 \lambda^2}\right] \quad . \tag{4}$$

In (4) X_i indicates the coordinate of the i flux line perpendicular to the direction of the twin boundaries (assumed to be all parallel to each other), x_k is the corresponding coordinate of the k twin boundary, V_0 is the parameter that determines the strength of the twin-boundary/flux-line interaction and the dimensionless parameter σ governs the range of that attraction. The range of the twin-boundary potential is expected to be short compared to the magnetic penetration depth λ and its strength to decrease fast; the functional form of the potential was therefore chosen to be a Gaussian. The numerical values of V_0 and σ are difficult to estimate and should be determined experimentally (*e.g.* from the pinning energies of the twin boundaries). In the calculations reported below the parameters were chosen so as to give results compatible with the experimental observations. The results were very insensitive to the choice of V_0 if the magnitude is larger than a given threshold (a change of two orders of magnitude in V_0 gave negligible changes in the *static* properties of the flux line

distributions, even though the *dynamic* properties may be considerably altered. The density and location of the twin boundaries are functions of the "quality" of the sample, and depend on the way the sample was fabricated.

If $U_0 = (\Phi_0)^2 / (8\pi^2\lambda^2)$ is taken to be the unit of energy per unit length of thickness of the sample, and λ is the unit of length, then the problem contains the following dimensionless parameters:

(i) Δf, the total excess flux line free energy in units of U_0;

(ii) $v_0 = V_0/U_0$, the strength of the twin-boundary/flux-line interaction in the new energy units;

(iii) L, the length of the chosen hexagonal unit cell, in units of λ;

(iv) l_f, the average separation between flux lines, in units of λ, in the perfect Abrikosov hexagonal lattice at a given value of the applied magnetic field; this quantity is a measure of the inverse value of the field that has penetrated the superconductor;

(v) N, the number of flux lines in the chosen unit cell, a quantity equal to $(L/l_f)^2$;

(vi) σ, the dimensionless range of the twin-boundary/flux-line attraction,

(vii) l_t, the average separation between twin boundaries in units of λ;

(viii) N_t, the number twin boundaries in the chosen unit cell, a quantity inversely proportional to l_t;

(ix) σ_t, the standard deviation for the distribution of twin boundary separations, in units of λ.

For weak magnetic fields ($H \gtrsim H_{c1}$) the average distance between the flux lines is larger than λ (*i.e.* $l_f > 1$), and the zeroth order Bessel function can be approximated by

$$K_0(R) \simeq [(\pi / (2R)]^{1/2} \exp(-R) \tag{5}$$

This leads to an interaction identical to a two-dimensional screened Coulomb repulsion. The total excess flux-line free energy now becomes

$$\Delta f = \sum_{i<j}^{N} \left[\frac{\pi}{2r_{ij}}\right]^{1/2} \exp\left[-r_{ij}\right] - v_0 \sum_{i}^{N} \sum_{k}^{N_{twins}} \exp\left[\frac{-(X_i - x_k)^2}{\sigma^2}\right] \tag{6}$$

This equation constitutes the basis of this work. The problem is to find the configurations of flux lines, for a given magnetic field and a given configuration of

twin boundaries that are local minima of the free-energy expression given above. Although some analytic methods have been attempted to solve this problem[11], it is far too complex to expect sensible solutions from that approach. The richness and variety of the numerical solutions reported below confirm this notion.

Before proceeding to report on the calculation and the results, the limitations of the model and approximations made should be discussed. The use of London's theory is probably a very good approximation, especially for the new high temperature superconductors since these materials all have a very large value of κ (≈ 100). The chosen form of the twin-boundary/flux-line interaction potential is a more difficult approximation to evaluate. Examination of the experimental data[9] clearly indicates that the interaction is attractive, and reasonably short-ranged. Therefore a Gaussian form, as adopted here, is plausible, although by no means certain. It can be justified qualitatively by assuming that the destruction of the order parameter (i.e. the formation of the core of the flux line) is more favorable at the twin boundary and its immediate neighborhood than in the rest of the crystal, and that there is negligible ineraction between the distribution of magnetic field lines and the twin boundaries themselves. In other words only when the core of the flux line lies within a few lattice parameters of the

twin boundary is the interaction appreciable.

III. MINIMIZATION AND RESULTS

The minimization of the free energy (6) was performed numerically. A hexagonal unit cell with periodic boundary condition was chosen, a given number of parallel twin boundaries was introduced and repeated periodically in the direction perpendicular to the boundaries, and a finite number of flux lines was placed at random in the hexagonal unit cell. This latter number was always a perfect square (4, 9, and 16). The flux lines were infinitesimally displaced and the values of (6) calculated at every stage until a local minimum was achieved. The procedure used a sequential quadratic programming algorithm, in which the search direction is the solution of a quadratic programming problem. By having a high accuracy in the calculations, the random initial start configuration "moved" to the "nearest" stable or metastable minimum configuration. The procedure for each twin-boundary configuration and for each N was repeated for 100 different initial random flux-line configurations.

Some features of the numerical procedure deserve comment. The unit cell was chosen to have hexagonal symmetry and only interactions between lines in the same

unit cell and in nearest-neighbor cells were included (longer-range interaction, between lines two or more cell away is always negligibly small for the screened coulomb potential).

The choice of hexagonal symmetry for the unit cell insured the natural hexagonal symmetry of the flux lattice in twin-free regions. Any other symmetry of the unit cell could in principle be chosen, but the boundary effects would produce unwanted structures unless the size were unreasonably large (and the computational tax excessive). The above choice was guaranteed to minimize size effects. In addition, because of the periodic boundary conditions, a favorable hexagonal Abrikosov lattice can only form if the number of flux lines is a perfect square. Any other choice would require one or more artificial defects of the flux lattice.

A stochastic function that generates a distribution of the N_{twins} twin boundaries in the unit cell must be defined. In the calculations a normal distribution was chosen, so that it gave an average separation of l_t, with a standard deviation σ_t. This means that, in the cases examined, by starting from any twin boundary and going in a direction perpendicular it, the average separation between twins is l_t, and the deviations from

this average are given by σ_t.

The initial distribution of flux lines was obtained from random-number generators. This procedure attempted to imitate the conditions in the decoration experiments[9,10] where the samples were field-cooled through the superconducting transition temperature to low temperatures of the experiment. The flux lines therefore were probably "nucleated" at random. Different results should be obtained in experiments where the field is applied after cooling to low temperatures, and the flux lines penetrate the sample "from one side". The initial random distribution mimics an ideal quenching, and probably overestimates the disorder in the final metastable states.

Calculation of a large number of random initial flux lattice configurations allows to compile, for a given set of parameters, statistical information on a variety of quantities: the density of metastable configurations; their distribution in energy; the flux distribution pair-correlation function.

In all calculations the following parameters were used:

$$v_0 = 0.05 \quad , \qquad L = 20 \quad ,$$
$$\sigma^2 = 0.05 \quad , \qquad (\sigma_t)^2 = 0.04 \quad .$$

The other parameters were varied, so that the following fifteen cases were studied

$$N = 4 \quad , \quad N = 9 \quad , \quad N = 16 \quad ;$$

$$N_{twins} = 0 \quad , \quad N_{twins} = 2 \quad , \quad N_{twins} = 4 \quad , \quad N_{twins} = 8 \quad , \quad N_{twins} = 18 \quad .$$

If the parameters of *YBaCuO* and the experimental results of Ref. 4 are used, these parameters correspond to magnetic fields of

$$B \approx 9.2\ G \quad , \quad B \approx 20.1\ G \quad , \quad B \approx 36.7\ G \quad ;$$

and twin-boundary separations of

$$\infty \quad , \quad 1.40\ \mu m \quad , \quad 0.70\ \mu m \quad , \quad 0.35\ \mu m \quad , \quad 0.16\ \mu m \quad ,$$

respectively. The penetration depth λ was taken[12,13] to be $0.14\ \mu m$.

The flux line decoration experiments[4,5] have been all, by necessity, performed at low magnetic fields. The numerical calculations reported here correspond, therefore, to low fields. For each value of the magnetic field and the distribution of twin boundaries the calculation was repeated 100 times, using new random initial configurations of the flux lines. For each of the fifteen cases, statistics of the energies and flux-line pair-correlation functions corresponding to the final (meta)stable states of the 100 initial configurations were obtained. Figures 1 - 4 show the histograms for the energy distributions of the twelve cases here considered that involve twin boundaries. Figures 5 - 9 exhibit the pair-correlation functions for the cases of N = 16, and N_{twins} equal to 0, 2, 4, 8, and 18 respectively. Figures 10 - 12 are examples of various stable and

metastable configurations.

When no twin boundaries are present, the flux lattice relaxes mostly to an Abrikosov lattice. Only defect-free Abrikosov lattices were obtained for all values of N reported here. However, for larger values of the magnetic field, structures involving an occasional flux-line-lattice dislocation were obtained: this was the situation when several cases for $N = 25$ were run.

When twin boundaries are present the metastable structures were very different. An analysis of the histograms in Figures 1 - 4 reveals that the energy distributions are essentially of three types:

1) Discrete, narrow, multimodal distributions observed when both the density of twin boundaries and the magnetic flux are low;

2) Quasi-continuous, single-mode distributions observed essentially when the density of twin boundaries is high;

3) Multimodal, broadened distributions in the intermediate regimes.

From an analysis of the histograms and the corresponding flux-line configurations it emerges that twin boundaries are attractive to flux lines only when they are popu-

lated by fewer lines than a critical number N_c per unit-cell length. For $N = 16$ and $N_{twins} = 2$ (see Figures 1 and 11) the critical number is five flux lines per unit-cell length, *i.e.* each twin boundary can accommodate up to five flux lines in the chosen unit cell. If the flux-line density (flux lines per unit cell) exceeds exceeds the product $N_{twins} \cdot N_c$, the additional lines are, by necessity, "caught" in the twin-boundary-free region. It is possible that, even though the twin boundaries are not saturated, some flux lines are nonetheless "caught" in the defect-free regions and produce thus a metastable, higher-energy state. This is the origin of the multimodal, discrete distributions observed. A clear example of this behavior is observed in Figures 10 and 1(a), where the four modes in the histogram correspond to 0, 1, 2 and 4 flux lines not located on twin boundaries. (Obviously 3 flux lines outside twin boundaries are also possible, even though our statistical sampling did not reach any of those cases). It should be noted that the highest-energy case in this example, Figure 10(d) and the right-most peak in Figure 1(a), correspond to a *perfect* Abrikosov lattice, which completely "ignores" the presence of the defects.

As seen in Figures 10-12, all metastable states tend to maximize the separation between neighboring lines. Since the lines are, however, bound to the twin

boundaries, there are competing processes which, to a varying degree, break the natural hexagonal symmetry.

This broken symmetry is evident in the flux-line pair-correlation diagrams of Figures 5 - 9. These figures correspond all to the same value of the magnetic field. In the case of a perfect crystal (Figure 5) the Abrikosov lattice yields a pair-correlation function consisting of 15 "spots" of equal strength in a perfect hexagonal pattern. Successive addition of twin boundaries tends to destroy the hexagonal symmetry, which is all but gone in Figures 8 and 9. Only average (statistical) mirror symmetries in the directions parallel and perpendicular to twin boundaries remain.

IV. CONCLUSIONS

The calculations reported here result in complicated metastable flux-line distributions in superconducting crystals with twin boundaries. There are, in this case, competing forces between the short-range attraction of flux lines and twin boundaries, and the repulsive (screened Coulomb) interaction between the flux lines. A large number of metastable configurations results in what may be called a "flux-line glass" situation, with different and sometimes contrasting behaviors which strongly depend on the den-

sities of flux lines (magnetic-filed strength) and twin boundaries (quality of the crystal).

The results reported here, based on calculations of small systems with periodic boundary conditions, should be considered as describing a small but macroscopic section of a much larger crystal. Envisioned that way, the patterns shown in the various figures here strongly resemble particular sections of the decoration experiments of references 4 and 9.

It should be mentioned also that the specific details of the patterns depend on the values of the force parameters chosen, in particular the form, range and strength of the twin-boundary flux-line attraction. The parameters adopted in the reported calculation are physically reasonable, and yield results which agree well with experimental obser-vations.

ACKNOWLEDGMENTS

One of us (HS) would like to acknowledge the financial support from: Carlsberg fondet (Denmark); Fabriksejer, Ingeniør Valdemar Selmer Trane og Hustru Elisa

Tranes Fund (Denmark). Knud Højgaard Fund (Denmark); NATO Fellowship Science Programme (Denmark); Otto Mønsteds Fond (Denmark); The Danish-American Foundation; Thomas B. Thriges Fund (Denmark); This research was supported, at the Lawrence Berkeley Laboratory, by the Director, Office of Energy Research, Office of Basic Energy Sciences, Materials Sciences Division, U.S. Department of Energy, under contract No. DE-AC03-76SF00098.

REFERENCES

1 A.A. Abrikosov, J. Exptl. Theoret. Phys. (U.S.S.R.) **32**, 1442 (1957). Sov. Phys. JETP **5**, 1174 (1957).

2 V. L. Ginzburg and L. D. Landau, Zh. Eksperim. i Teor. Fiz **20** , 1064 (1950).

3 See for example M. Tinkham; *Introduction to superconductivity*. (McGraw-Hill, New York, 1975), Chapter 5.

4 P.L. Gammel, D.J. Bishop, G.J. Dolan, J.R. Kwo, C.A. Murry, L.F. Schneemyer, and J.V. Waszczak, Phys. Rev. Lett. **59** , 2592 (1987).

5 P.L. Gammel, L.F. Schneemyer, J.V. Waszczak, and D.J. Bishop, Phys. Rev. Lett., **61** , 1666 (1988).

6 D.R. Nelson, Phys. Rev. Lett. **60** , 1973 (1988).

7 D.R. Nelson and H.S. Seung, Phys. Rev. B, **39** , 9153 (1989).

8 M.P.A. Fisher, Phys. Rev. Lett. **62** , 1415 (1989).

9 G.J. Dolan, G.V. Chandrashekhar, T.R. Dinger, C. Feild, and F. Holtzberg, Phys. Rev. Lett. **62** , 827 (1989).

10 G.J. Dolan, F. Holtzberg, C. Feild, and T.R. Dinger, Phys. Rev. Lett. **62** , 2184 (1989).

11 E. H. Brandt, Phys. Rev. Lett. **63** , 1106 (1989), and references therein.

12 L. Krusin-Elbaum, R.L. Greene, F. Holtzberg, A.P. Malozemoff, and Y. Yeshurun, Phys. Rev. Lett. **62** , 217 (1989).

13 With this value of λ, the unit-cell length in these calculations is $L = 2.8\ \mu m = 20\lambda$.

FIGURE CAPTIONS

Figure 1

Histogram of the energy distribution of 100 cases with random initial conditions corresponding to 2 twin boundaries in the unit cell, for a flux-line density of (a) 4 lines per unit cell; (b) 9 lines per unit cell; and (c) 16 lines per unit cell. The energies are in units of U_0, defined in the text.

Figure 2

Histogram of the energy distribution of 100 cases with random initial conditions corresponding to 4 twin boundaries in the unit cell, for a flux-line density of (a) 4 lines per unit cell; (b) 9 lines per unit cell; and (c) 16 lines per unit cell. The energies are in units of U_0, defined in the text.

Figure 3

Histogram of the energy distribution of 100 cases with random initial conditions corresponding to 8 twin boundaries in the unit cell, for a flux-line density of (a) 4 lines per unit cell; (b) 9 lines per unit cell; and (c) 16 lines per unit cell. The energies are in

units of U_0, defined in the text.

Figure 4

Histogram of the energy distribution of 100 cases with random initial conditions corresponding to 18 twin boundaries in the unit cell, for a flux-line density of (a) 4 lines per unit cell; (b) 9 lines per unit cell; and (c) 16 lines per unit cell. The energies are in units of U_0, defined in the text.

Figure 5

The pair-correlation function corresponding to the perfect crystal (no twin boundaries) and 16 flux lines per unit cell. The pattern is a set of sixteen delta functions with perfect hexagonal symmetry.

Figure 6

The pair-correlation function for the 100 cases corresponding to 2 twin boundaries and 16 flux lines per unit cell. The pattern exhibits mirror symmetry and distorted but clear hexagonal symmetry.

Figure 7

The pair-correlation function for the 100 cases corresponding to 4 twin boundaries and 16 flux lines per unit cell. The pattern exhibits mirror symmetry and distorted but clear and pronounced hexagonal symmetry

Figure 8

The pair-correlation function for the 100 cases corresponding to 8 twin boundaries and 16 flux lines per unit cell. The pattern exhibits essentially only mirror symmetry.

Figure 9

The pair-correlation function for the 100 cases corresponding to 18 twin boundaries and 16 flux lines per unit cell. The pattern exhibits mirror symmetry and, with the exception of a repulsive, distorted "hard core", much less pronounced features and an essentially uniform distribution

Figure 10

Four characteristic local-minimum flux-line arrangements corresponding to 2 twin boundaries and 4 flux lines per unit hexagonal cell. (a) A minimum-energy pattern with the 4 flux lines lying on the twin boundaries and forming a distorted Abrikosov hexagonal lattice. (b) An intermediate-energy, distorted hexagonal pattern with only one line not on a twin boundary. (c) A higher-energy arrangement of distorted hexagonal symmetry, with 2 lines on twin boundaries and the other 2 caught in between. (d) A very-high-energy metastable structure, a perfect Abrikosov hexagonal lattice, with all 4 lines caught self-consistently away from twin boundaries.

Figure 11

A typical metastable configuration corresponding to 2 twin boundaries and 16 flux lines. Nine flux lines lie on the twin boundaries and and seven far from them. The twin boundaries are highly "populated" and have become repulsive to the other lines. This is a typical pattern observed experimentally when the density of twin boundaries is relatively low and the magnetic flux is relatively high.

Figure 12

A typical metastable configuration corresponding to 18 twin boundaries and 16 flux lines. All flux lines lie on the twin boundaries. The twin boundaries are only sparsely "populated" and can accommodate more lines. This is a typical pattern observed experimentally when the density of twin boundaries is relatively high and the magnetic flux is relatively low.

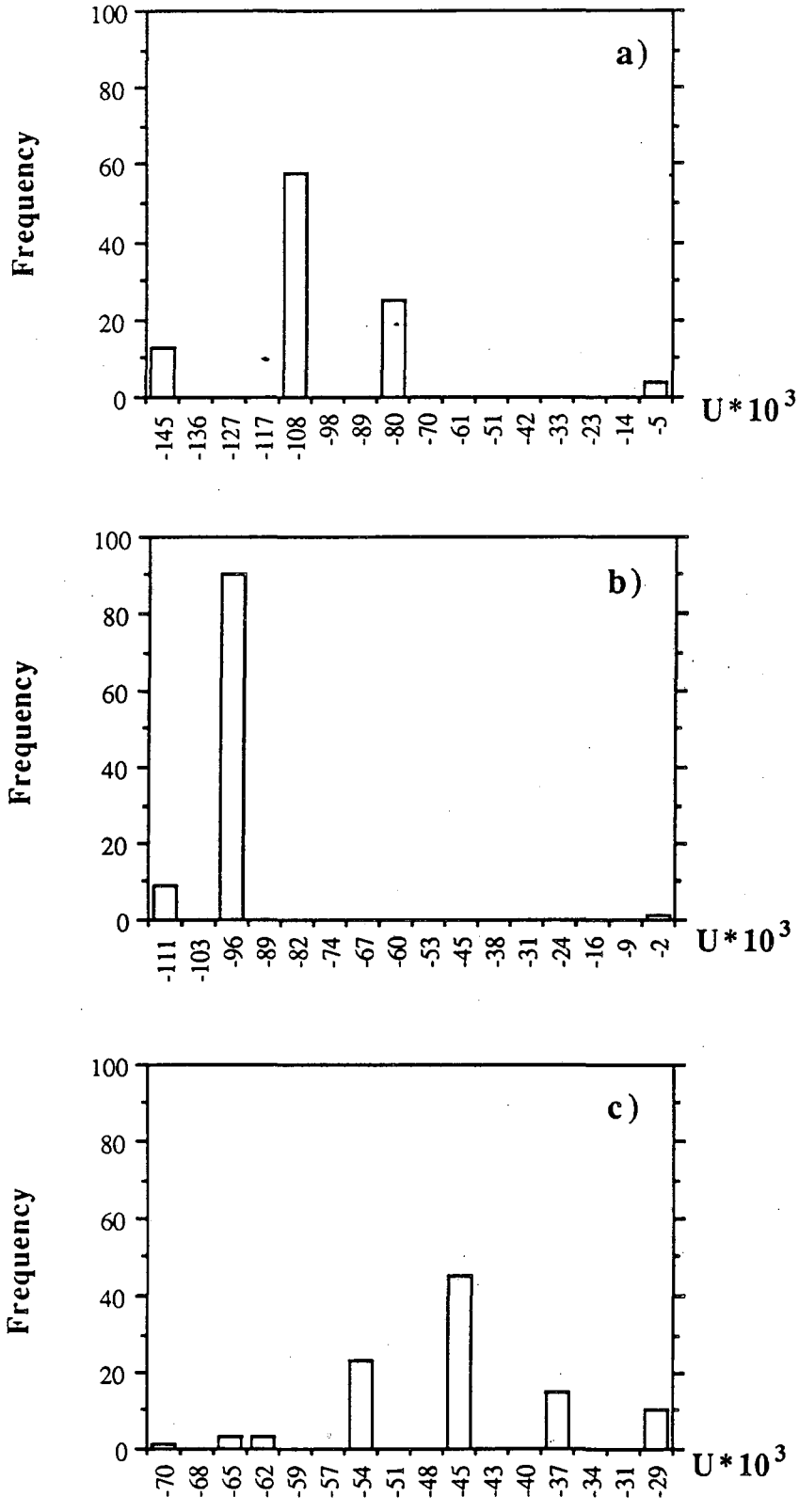
a)
Frequency
100
80
60
40
20
0
-145
-136
-127
-117
-108
-98
-89
-80
-70
-61
-51
-42
-33
-23
-14
-5
U*10^3
b)
Frequency
100
80
60
40
20
0
-111
-103
-96
-89
-82
-74
-67
-60
-53
-45
-38
-31
-24
-16
-9
-2
U*10^3
c)
Frequency
100
80
60
40
20
0
-70
-68
-65
-62
-59
-57
-54
-51
-48
-45
-43
-40
-37
-34
-31
-29
U*10^3

Figure 1

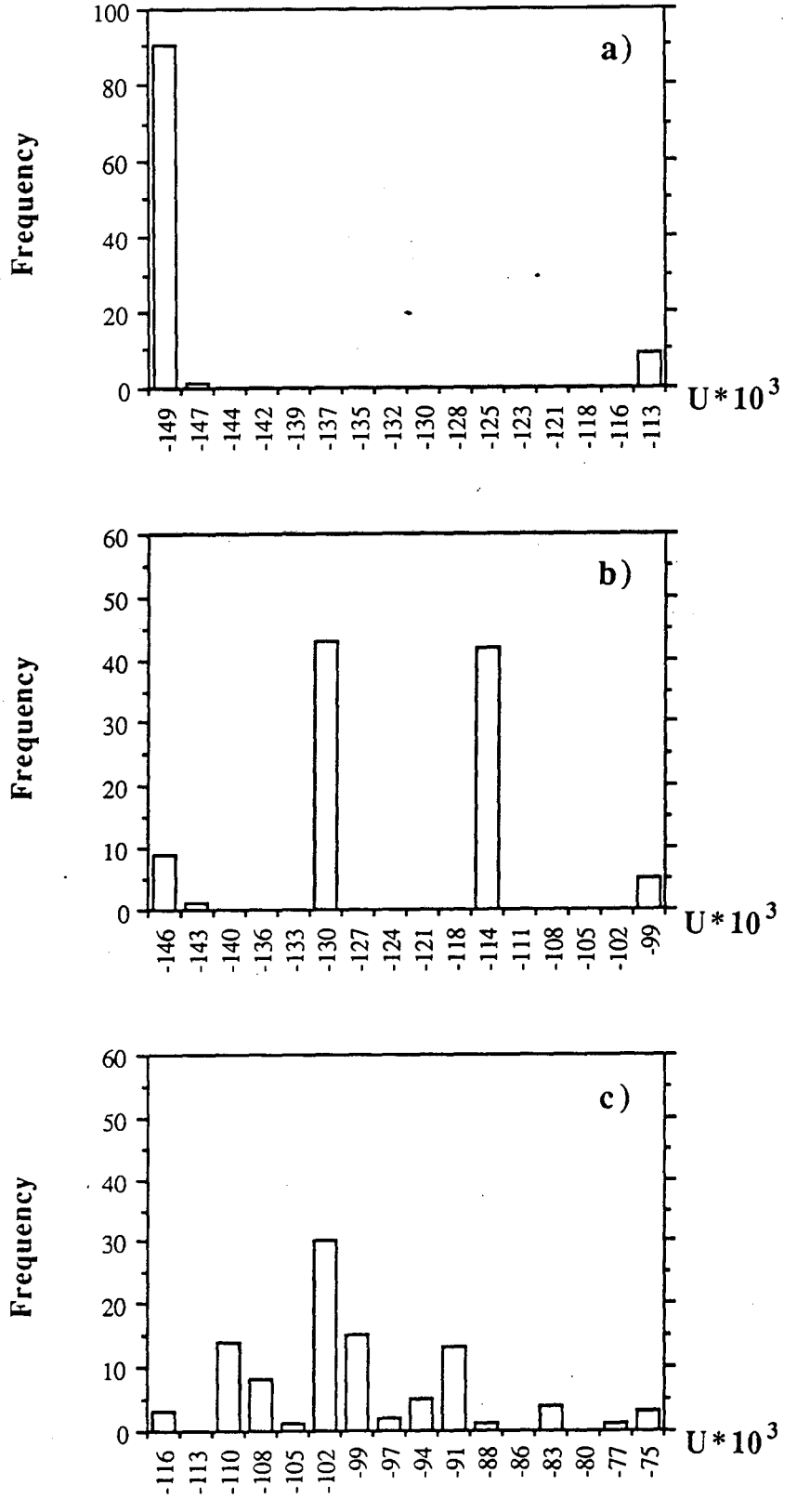
a)
Frequency
100
80
60
40
20
0
-149
-147
-144
-142
-139
-137
-135
-132
-130
-128
-125
-123
-121
-118
-116
-113
U*10^3
b)
Frequency
60
50
40
30
20
10
0
-146
-143
-140
-136
-133
-130
-127
-124
-121
-118
-114
-111
-108
-105
-102
-99
U*10^3
c)
Frequency
60
50
40
30
20
10
0
-116
-113
-110
-108
-105
-102
-99
-97
-94
-91
-88
-86
-83
-80
-77
-75
U*10^3

Figure 2

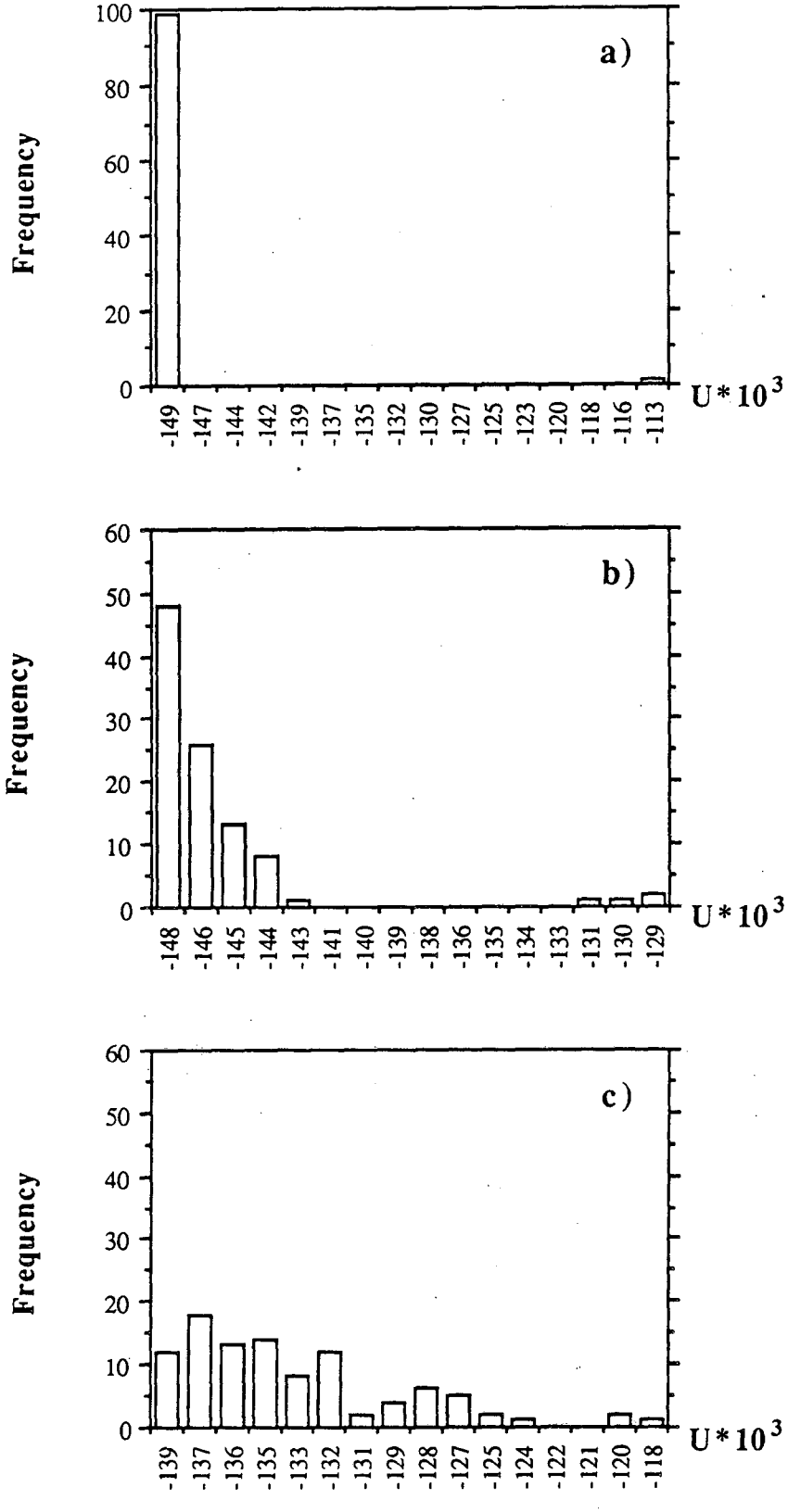
a)
Frequency
100
80
60
40
20
0
-149
-147
-144
-142
-139
-137
-135
-132
-130
-127
-125
-123
-120
-118
-116
-113
U*10^3
b)
Frequency
60
50
40
30
20
10
0
-148
-146
-145
-144
-143
-141
-140
-139
-138
-136
-135
-134
-133
-131
-130
-129
U*10^3
c)
Frequency
60
50
40
30
20
10
0
-139
-137
-136
-135
-133
-132
-131
-129
-128
-127
-125
-124
-122
-121
-120
-118
U*10^3

Figure 3

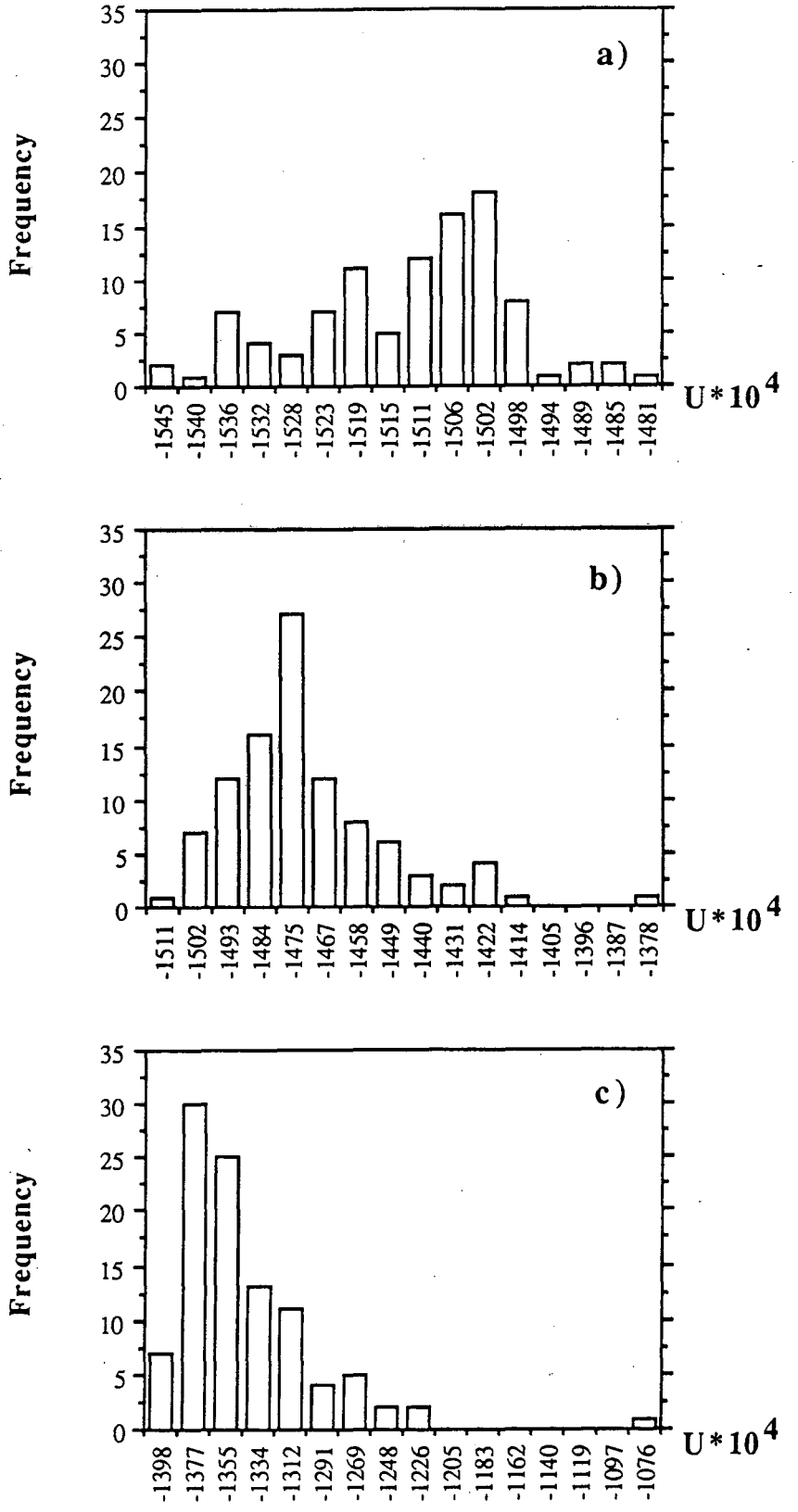
a)
Frequency
35
30
25
20
15
10
5
0
-1545
-1540
-1536
-1532
-1528
-1523
-1519
-1515
-1511
-1506
-1502
-1498
-1494
-1489
-1485
-1481
U*10^4
b)
Frequency
-1511
-1502
-1493
-1484
-1475
-1467
-1458
-1449
-1440
-1431
-1422
-1414
-1405
-1396
-1387
-1378
U*10^4
c)
Frequency
-1398
-1377
-1355
-1334
-1312
-1291
-1269
-1248
-1226
-1205
-1183
-1162
-1140
-1119
-1097
-1076
U*10^4

Figure 4

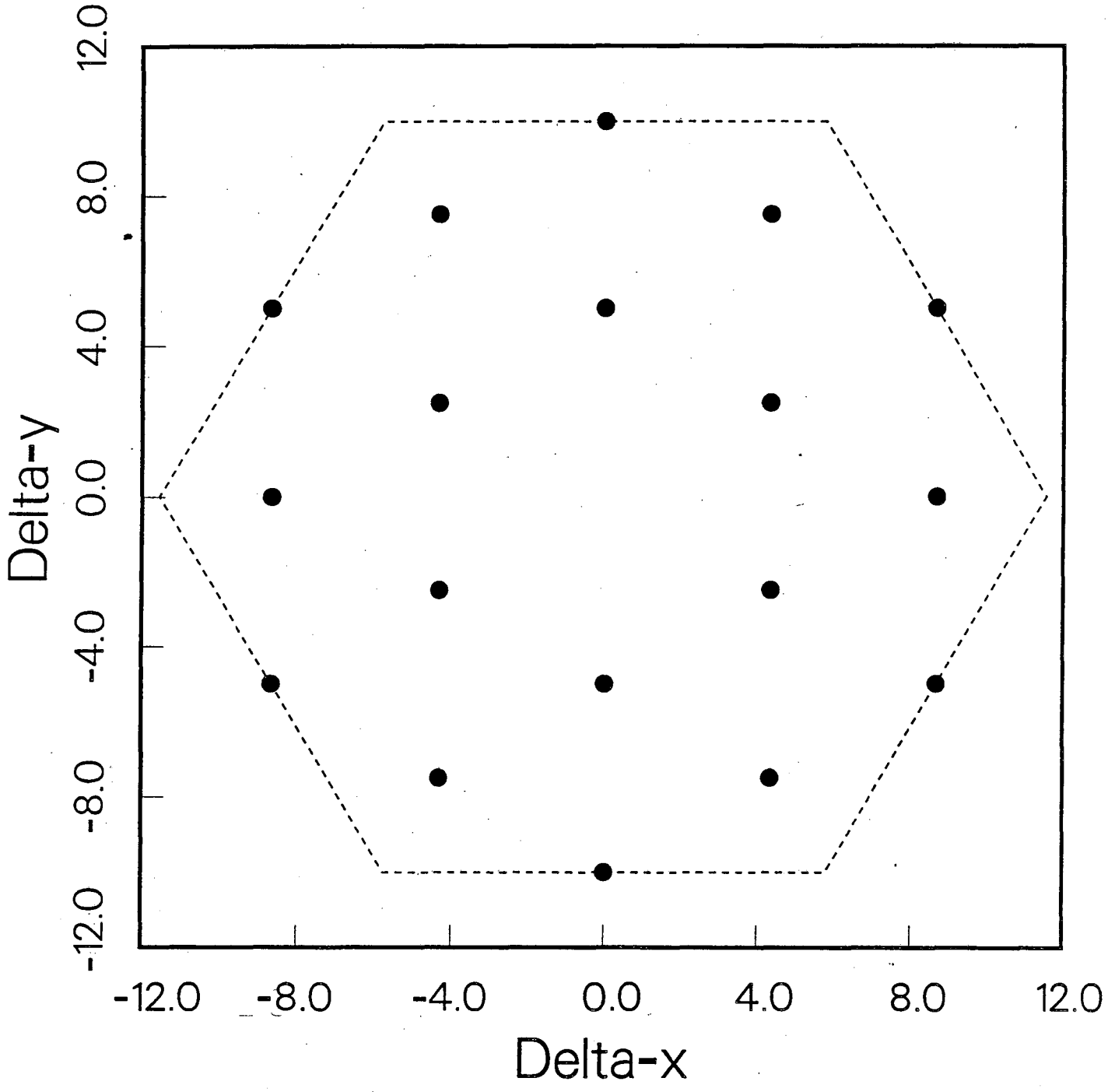

Figure 5

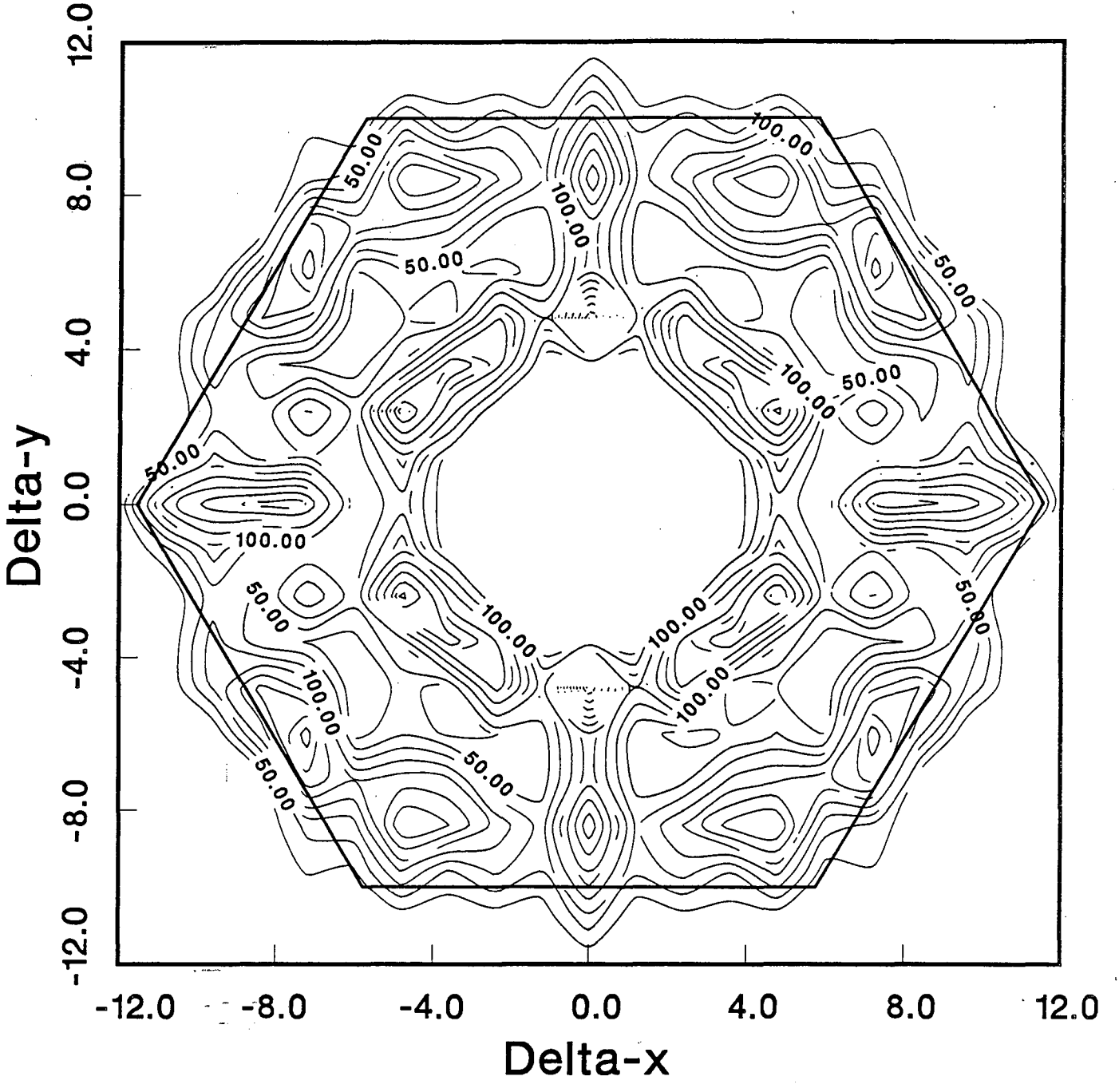
12.0
8.0
4.0
0.0
-4.0
-8.0
-12.0
Delta-y
-12.0
-8.0
-4.0
0.0
4.0
8.0
12.0
Delta-x
50.00
100.00

Figure 6

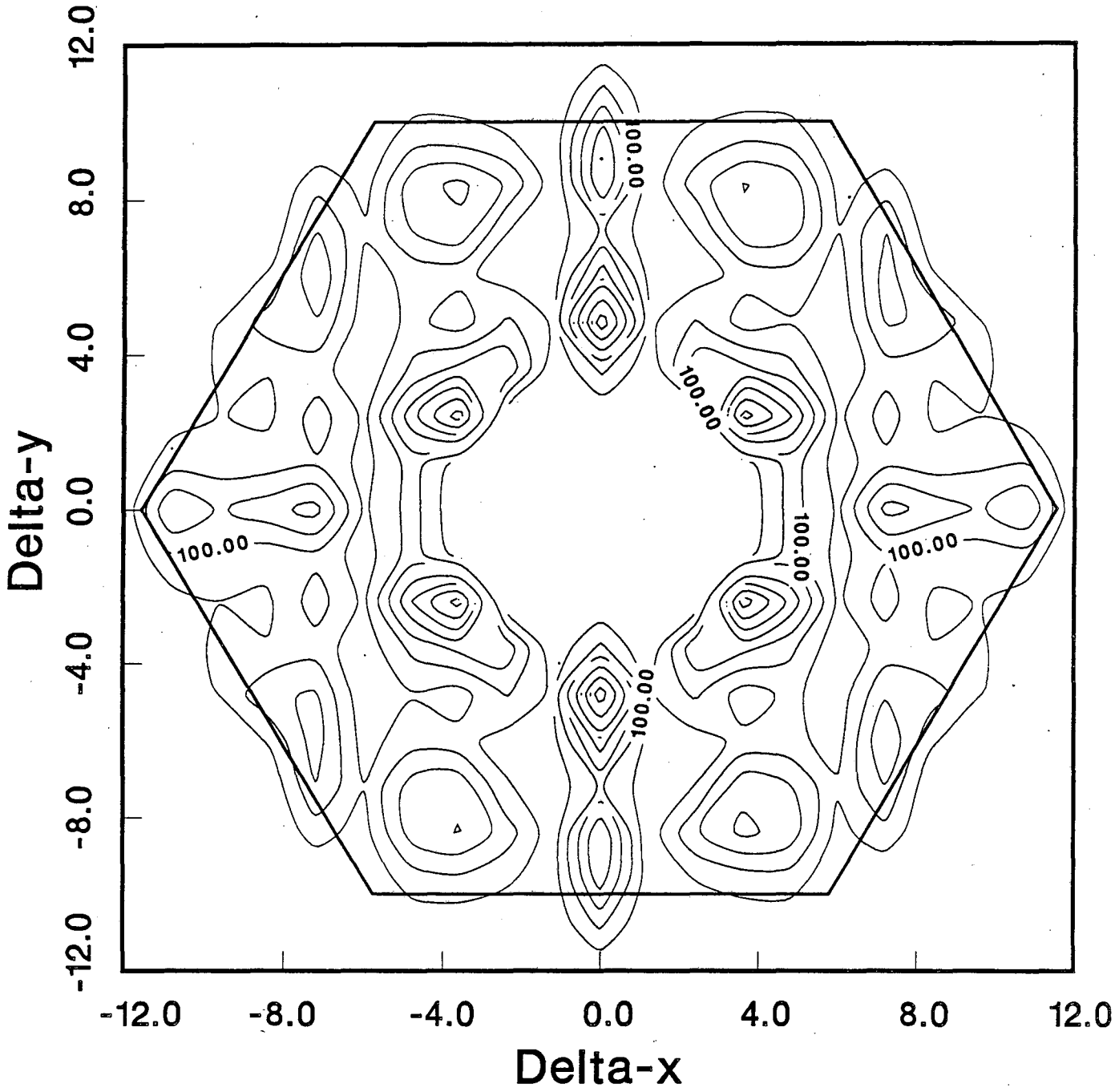
12.0
8.0
4.0
0.0
-4.0
-8.0
-12.0
Delta-y
-12.0
-8.0
-4.0
0.0
4.0
8.0
12.0
Delta-x
100.00
100.00
100.00
100.00
100.00
100.00

Figure 7

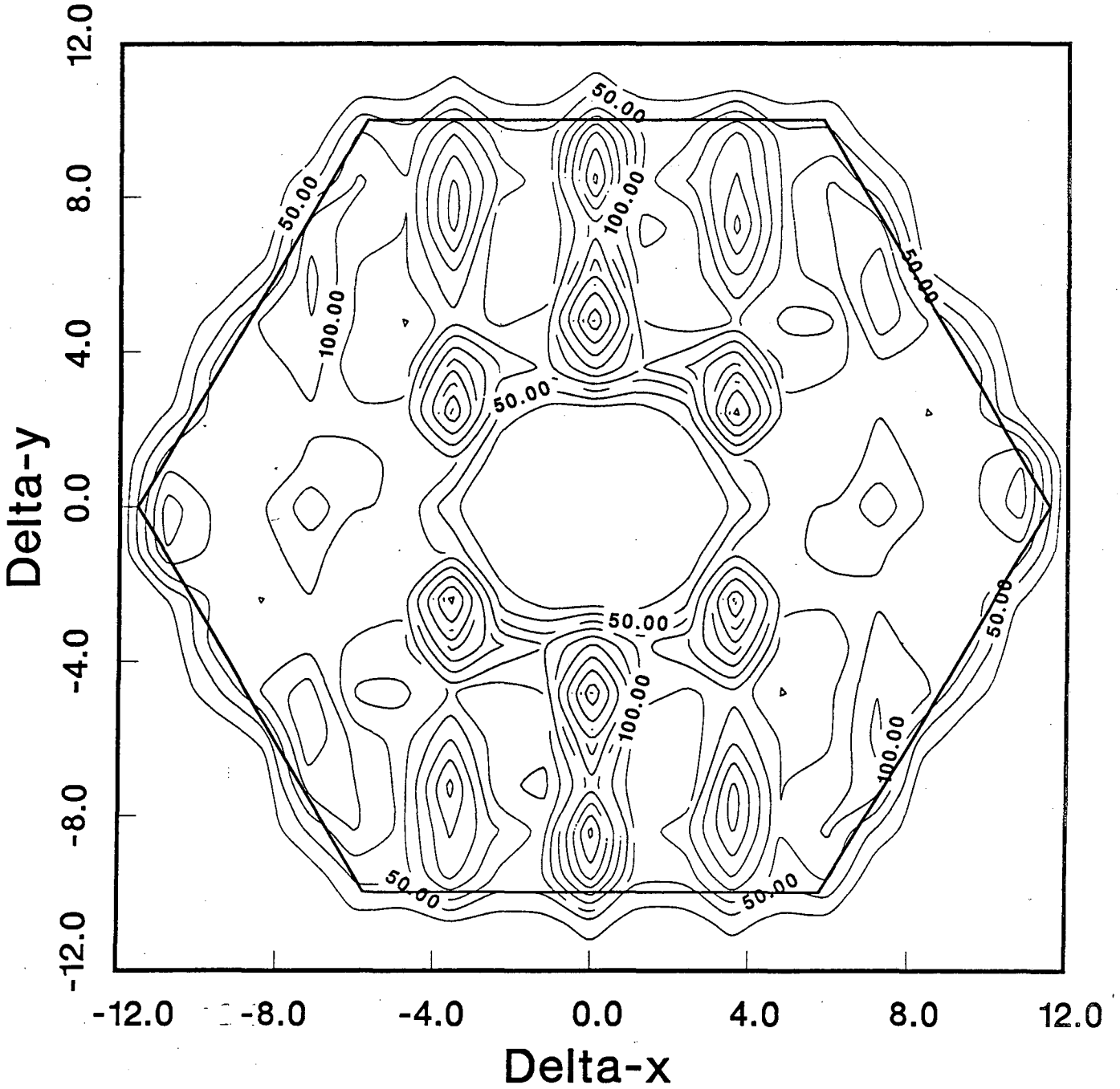
12.0
8.0
4.0
0.0
-4.0
-8.0
-12.0
Delta-y
-12.0
-8.0
-4.0
0.0
4.0
8.0
12.0
Delta-x
50.00
100.00
50.00
100.00
50.00
50.00
100.00
50.00
50.00
100.00
50.00
100.00
50.00

Figure 8

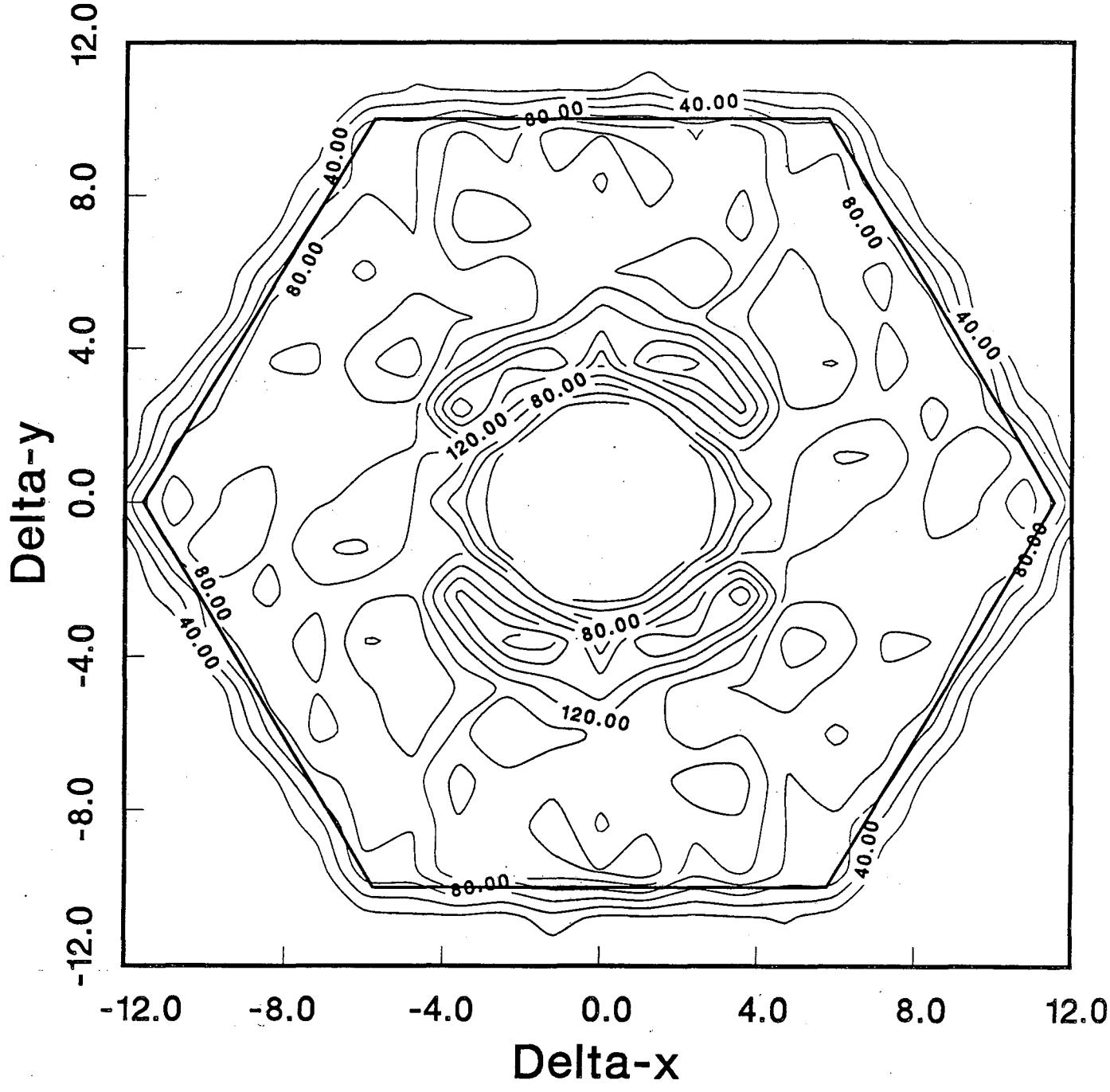
12.0
8.0
4.0
0.0
-4.0
-8.0
-12.0
Delta-y
-12.0
-8.0
-4.0
0.0
4.0
8.0
12.0
Delta-x
40.00
80.00
120.00

Figure 9

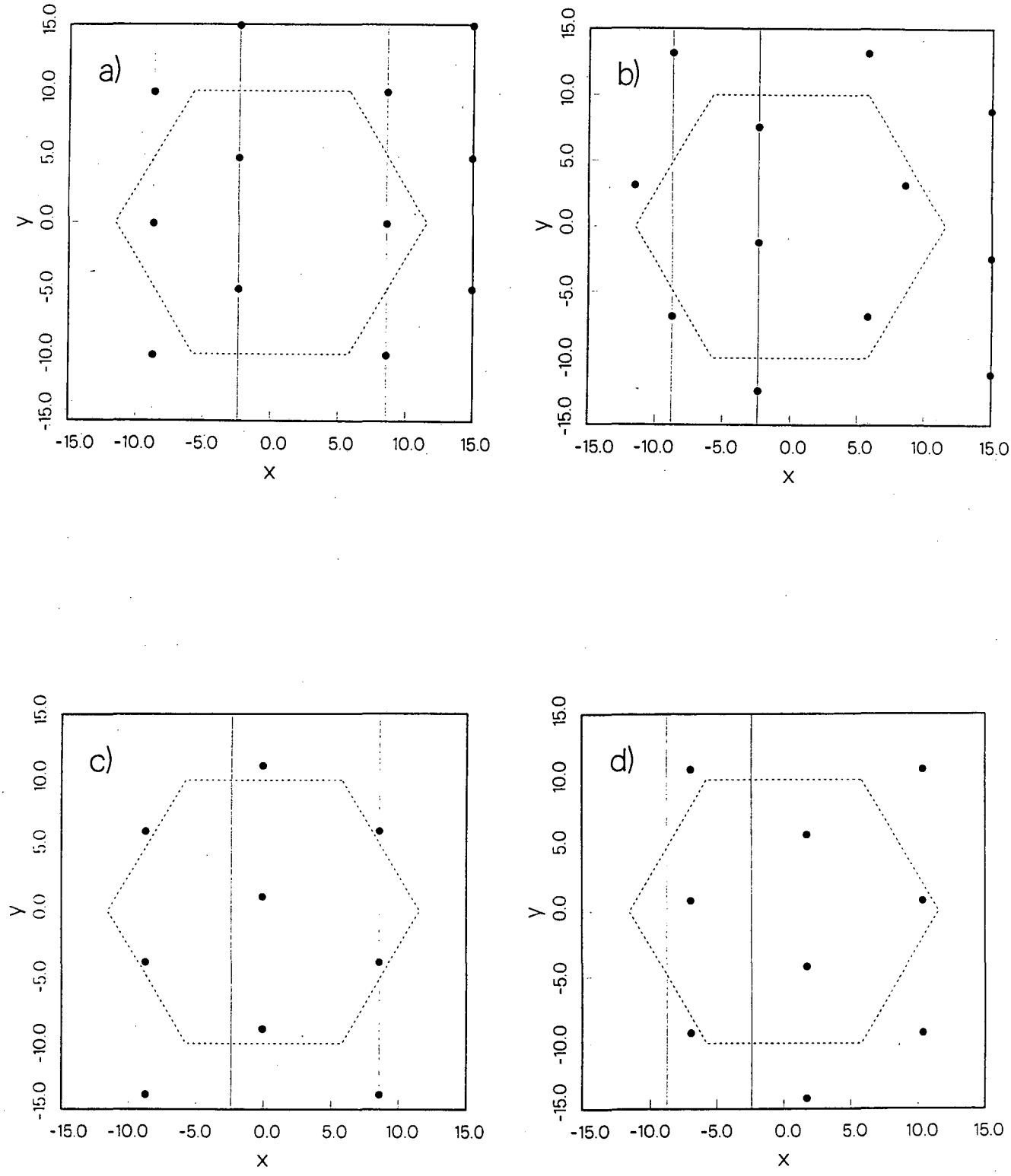

Figure 10

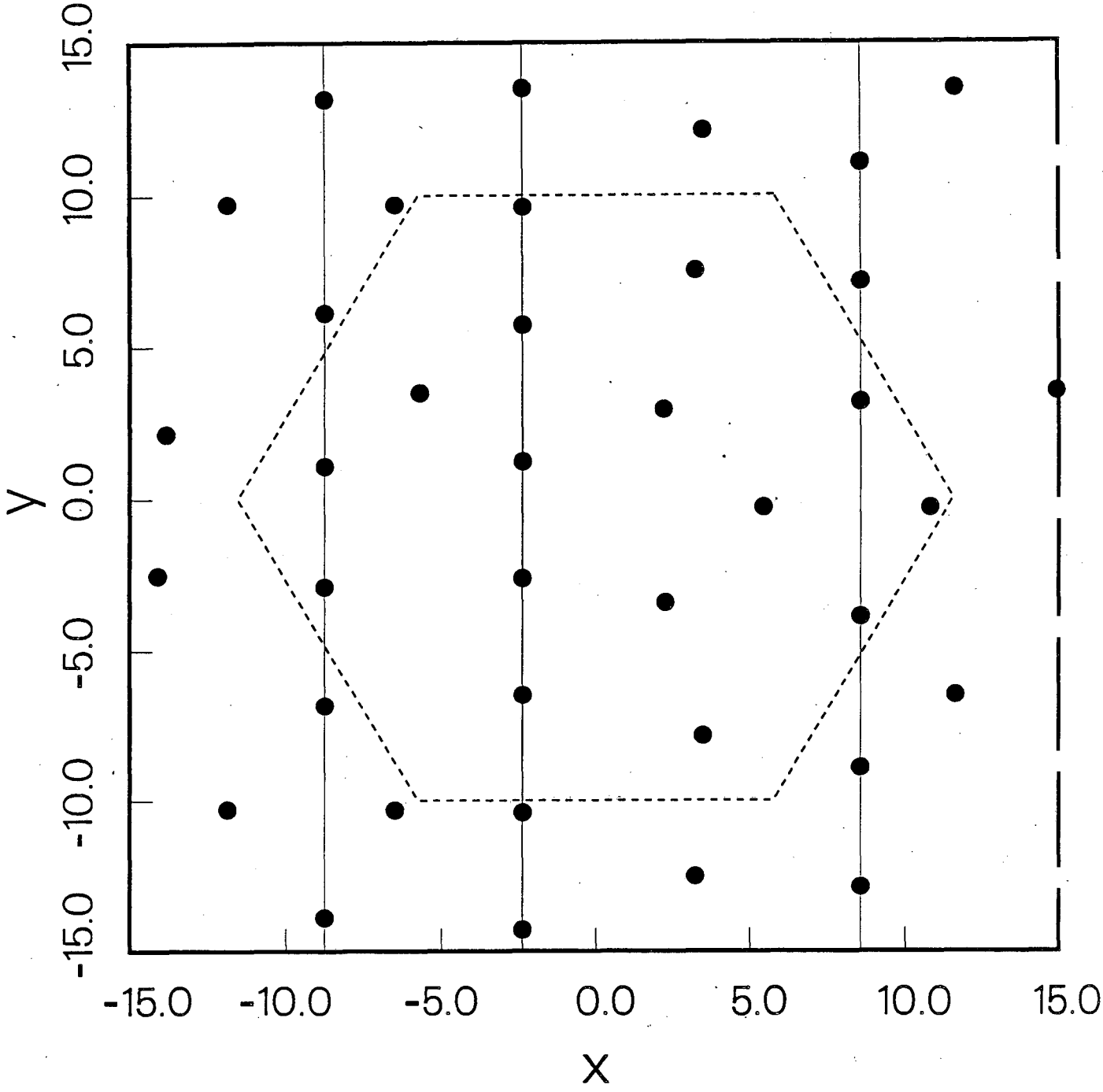

Figure 11

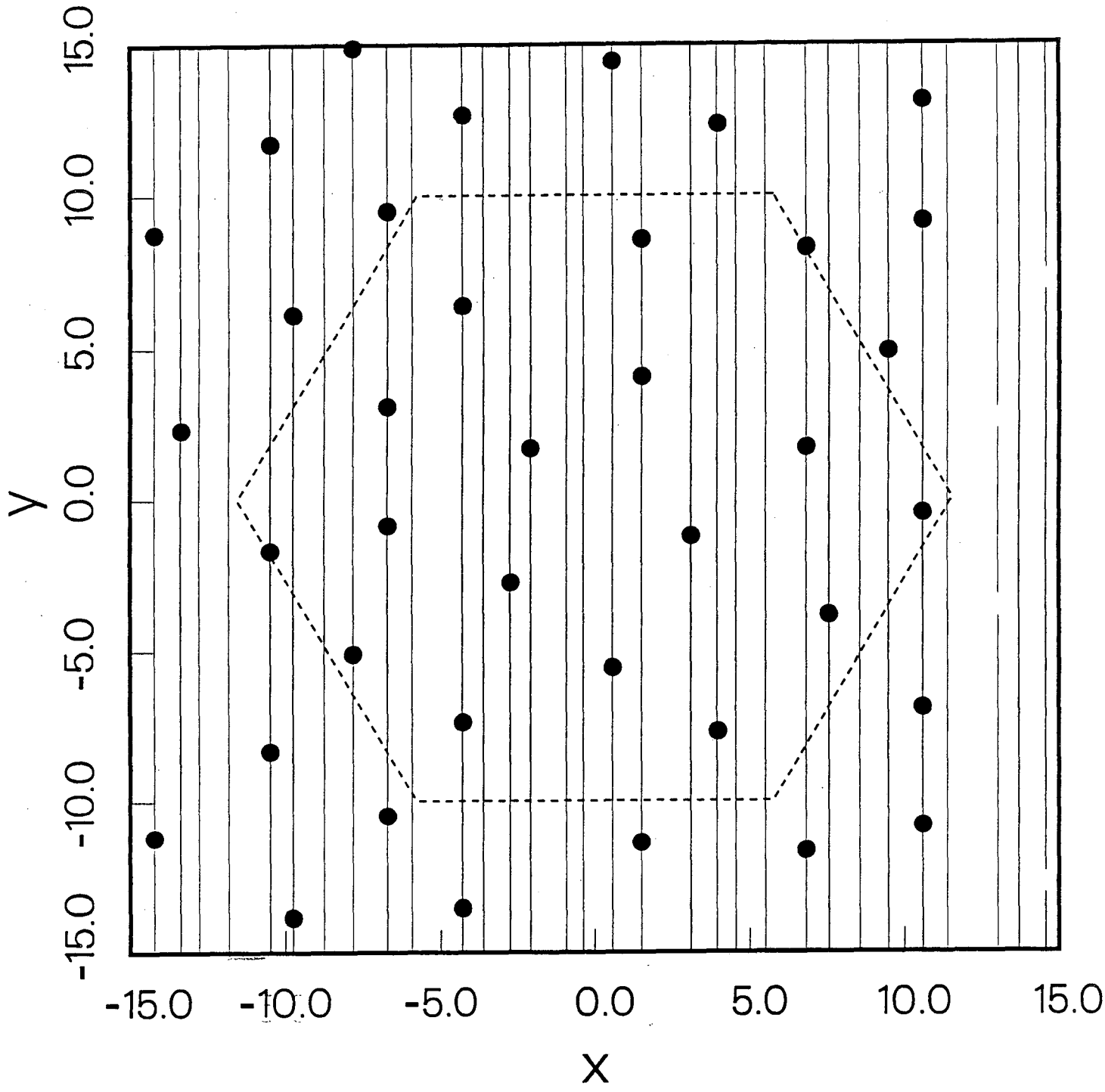

Figure 12

LAWRENCE BERKELEY LABORATORY
TECHNICAL INFORMATION DEPARTMENT
1 CYCLOTRON ROAD
BERKELEY, CALIFORNIA 94720